1 Calibration against independent human travel datasets

1.1 Calibration against United States Bureau of Transportation Statistics Data

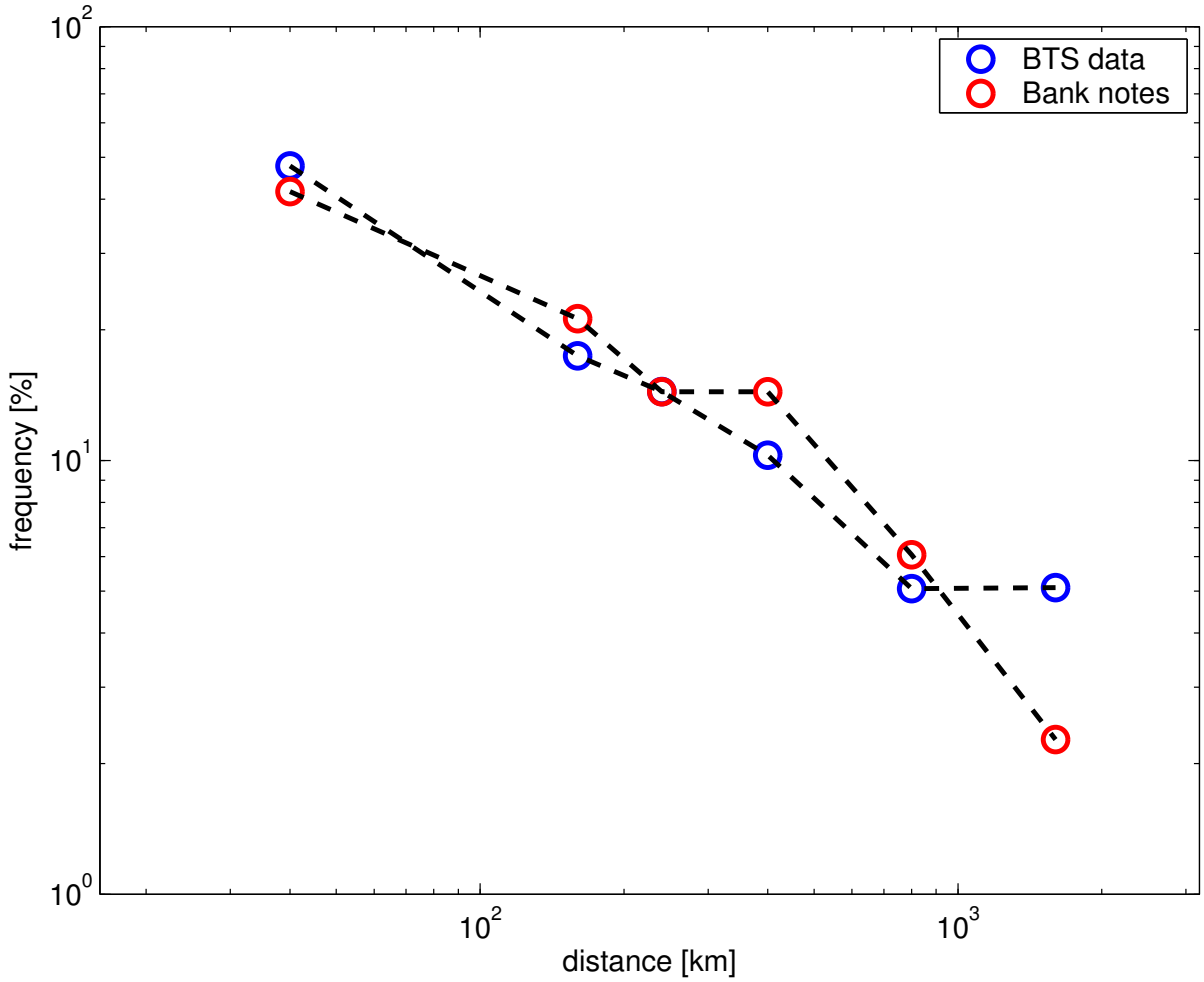

Figure 1.1: Histograms comparing the travelling data published by the BTS with short time bank note dispersal. The symbols denote the percentage of distances travelled within the limits of the categories listed in table 1.1 as a function of the lower bound of the distance bins.

Along an independent line we have compared our results to data published by the United States Bureau of Transportation Statistics (BTS, www.bts.gov). The BTS has evaluated 2,617,126 round trip distances of at least 50 miles. Details of the survey can be found in Table 1-39 in the section *National Transportation Statistics* at www.bts.gov. Although the BTS dataset is large, the movements were histogrammed

with a low spatial resolution: The distances d travelled were grouped into bins:

$$\begin{array}{rcl} 25\,\text{miles} & < d < & 100\,\text{miles} \\ 100\,\text{miles} & < d < & 150\,\text{miles} \\ 150\,\text{miles} & < d < & 250\,\text{miles} \\ 250\,\text{miles} & < d < & 500\,\text{miles} \\ 500\,\text{miles} & < d < & 1000\,\text{miles} \\ 1000\,\text{miles} & < d & \end{array} \tag{1.1}$$

We have computed the same histogram from the short time ($\Delta t < 2$ days) bank note dispersal, the results of which are shown in Fig. 1.1. The BTS data agrees well with the bank note dispersal data, thus confirming our results. We would like to point out, that our data permits a much higher spatial resolution than those published by the BTS.

1.2 Correlation of bank note transport and long distance aviation travel

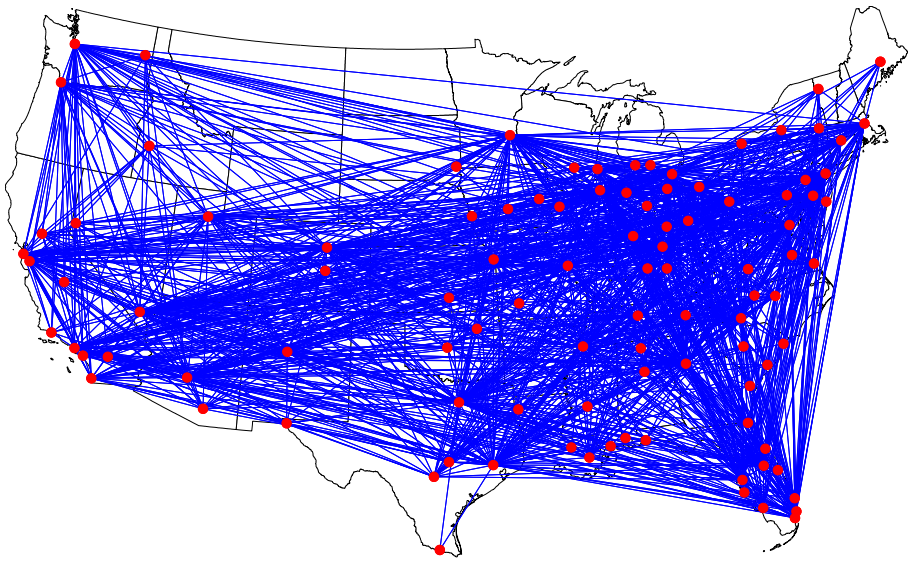

Figure 1.2: The civil aviation network of the United States. The 102 largest airports are depicted by red symbols. Blue lines represent connections between airports. The entire network consists of 2,743 weighed connections transporting approximately 3.9 million passengers per day.

In order to verify our results we compared the transport of bank notes with passenger flux on the US aviation network (Fig. 1.2). In this comparison we considered approx. 95% of the entire US-aviation network. This network can be represented by a matrix W each element W_{ij} of which represents the number of passengers travelling between airport i and j per unit time. The network represents a subnetwork of the entire worldwide aviation network which was recently employed in a study of the worldwide spread of human infectious disease [1].

The flux matrix W_{ij} represents an approximate measure for the short time travelling behavior of humans on large geographical scales between urban areas in the United States. If the inference from bank note dynamics to humans is valid, one expects the matrix W_{ij} to correlate significantly with the flux of bank notes between nodes i and j. The transport of bank notes can be represented by a matrix element M_{ij}, i.e. the number of bank notes which travelled from i to j in a short period of time Δt. This number

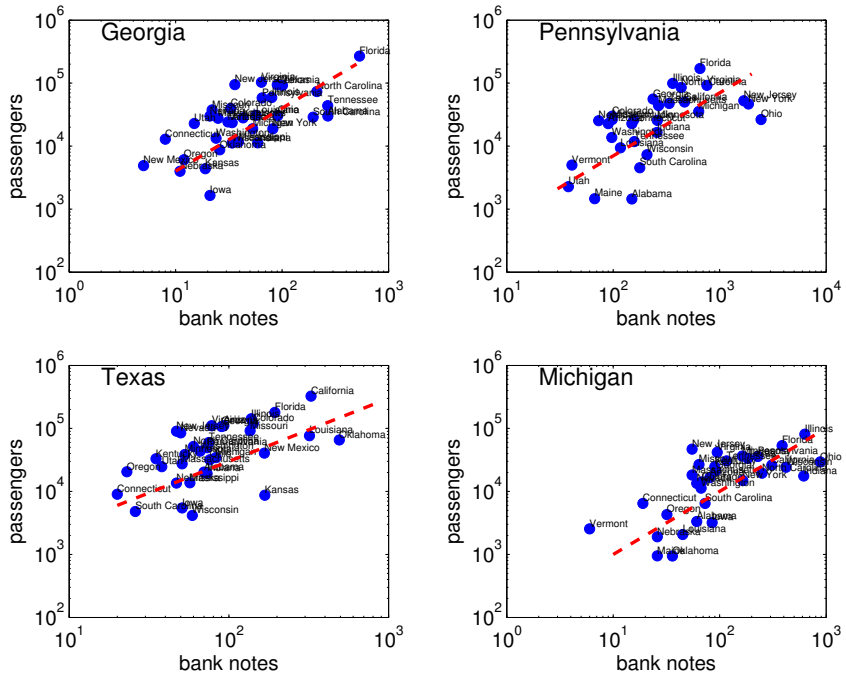

Figure 1.3: The correlation between human long distance travel and short time bank note transport. For the states n =Georgia, Pennsylvania, Texas and Michigan each panel depicts the number of passengers $\tilde{W}_{mn}$ travelling to target states per day versus the number of bank notes $\tilde{M}_{mn}$ transported within a time interval $\Delta t = 4$ weeks (blue symbols). The red dashed line represents a linear relationship.

can be extracted from our bill tracking dataset. In order to obtain reliable statistics, we computed the flux of passengers on one hand and bank notes on the other between 48 states. For each state n we determined the number of passengers $\tilde{W}_{mn}$ and bank notes $\tilde{M}_{mn}$ which travelled to state m from the underlying matrices W_{ij} and M_{ij}, respectively.

Fig. 1.3 depicts scatter plots of $\tilde{W}_{mn}$ versus $\tilde{M}_{mn}$ for four representative states, i.e. n =Georgia, Pennsylvania, Texas and Michigan on a log-log scale. Flux elements for which either $\tilde{M}_{mn} = 0$ or $\tilde{W}_{mn} = 0$ we excluded. Apart from fluctuations, the scatter plots are in agreement with a linear relation between human and bank note dispersal which supports the idea put forward in this work. Of course, an exact proportionality can not be expected. For example passenger flux between geographically adjacent states is less than bank note flux as bank notes primarily travel by other means of transportation (car, train) between such states. On the other hand, passenger flux to an airport with a catchment area overlapping with a number of geographically small but highly populated states (New England States such as Rhode Island, Delaware, etc.) is larger than the associated bank note dispersal. In order to obtain a significant flux of bank notes we had to increase the inter report time interval to four weeks. Despite these and other error sources, the correlation is significantly positive.

The degree of correlation can be quantified by the correlation coefficient

$$R = \frac{\left\langle \tilde{W}_{mn}\,\tilde{M}_{mn} \right\rangle - \left\langle \tilde{W}_{mn} \right\rangle \left\langle \tilde{M}_{mn} \right\rangle}{\sqrt{(\left\langle \tilde{W}_{mn}^2 \right\rangle - \left\langle \tilde{W}_{mn} \right\rangle^2)\,(\left\langle \tilde{M}_{mn} \right\rangle - \left\langle \tilde{M}_{mn} \right\rangle^2)}}. \tag{1.2}$$

For perfectly correlated and anti-correlated quantities $R = 1$ and $R = -1$, respectively. For statistically independent variables $R = 0$. The correlation coefficient for all 48 States individually and together is

listed in Table 1. The transport of passengers and bank notes to all other states exhibit a significant degree of correlation with an overall correlation coefficient of approximately 0.5.

State	R	**# target states** m	**State**	R	**# target states** m
All States	**0.47**	**882**			
Illinois	0.51	37	Connecticut	0.03	17
Kentucky	0.57	36	New Mexico	0.42	16
Georgia	0.67	34	Nebraska	0.73	16
Texas	0.57	33	Oklahoma	0.69	15
New Jersey	0.57	33	Alabama	0.69	15
Minnesota	0.47	33	Iowa	0.64	13
Arizona	0.68	33	South Carolina	0.64	10
Missouri	0.24	32	Kansas	0.50	10
Michigan	0.69	32	Vermont	-0.30	9
Nevada	0.79	31	Idaho	0.45	9
Colorado	0.53	31	Mississippi	0.39	8
Florida	0.68	30	Maine	0.34	7
Tennessee	0.67	29	South Dakota	0.93	4
Pennsylvania	0.62	29	Wyoming	-	-
North Carolina	0.67	27	West Virginia	-	-
Massachusetts	0.40	26	Rhode Island	-	-
California	0.63	26	North Dakota	-	-
Ohio	0.53	25	New Hampshire	-	-
Wisconsin	0.31	23	Montana	-	-
Washington	0.49	23	Maryland	-	-
Utah	0.50	21	Delaware	-	-
Indiana	0.21	21	Arkansas	-	-
Louisiana	0.63	20			
New York	0.57	17			

Table 1.1: The correlation between long distance travel and short time bank note transport. For each state n and the set of connected target states (i.e. those states m for which both $\tilde{W}_{mn}$ and $\tilde{M}_{mn}$ are nonzero) the correlation coefficient (Eq. 1.2) is computed. For all states the correlation is significantly positive as well as for the entire set of flux connection $n \to m$ (ensemble size: 882).

Bibliography

[1] L. Hufnagel, D. Brockmann, and T. Geisel, *Forecast and control of epidemics in a globalized world*, PNAS **101** (2004), 15124–15129.

1 Lévy flights and continuous time random walks (CTRW)

1.1 Random walks and Lévy flights

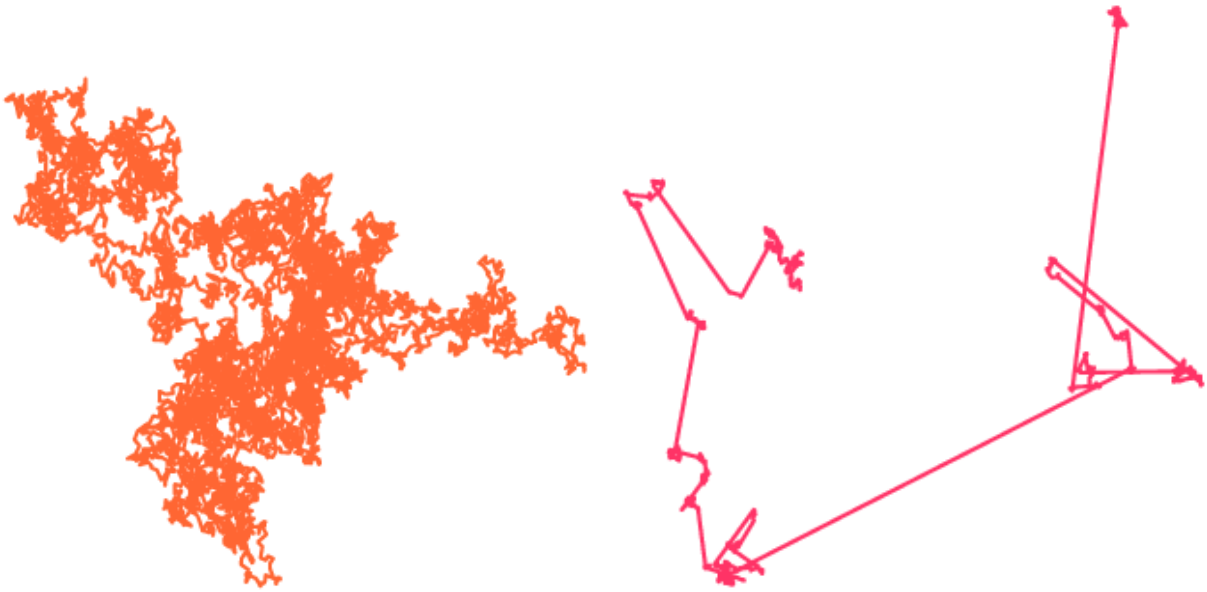

Figure 1.1: Two dimensional trajectories of random walks on large scales. Left: Ordinary random walk with finite, well defined variance of single steps. Right: A Lévy flight trajectory of index $\beta = 1$.

The position of an ordinary random walk is frequently defined as a sum of N independent identically distributed displacements ΔX_n:

$$X_N = \sum_{n=1}^{N} \Delta X_n. \tag{1.1}$$

Each displacement is drawn from the same probability density function (pdf) $p(\Delta x)$. Here it suffices to discuss symmetric single step pdfs in one dimension. According to the central limit theorem the pdf $W_Y(y, N)$ for the scaled position

$$Y_N = \frac{X_N}{\sqrt{N}} \tag{1.2}$$

is independent of N in the limit $N \to \infty$ and Gaussian, i.e.

$$\lim_{N\to\infty} W_Y(y, N) = W_Y(y) = \frac{1}{\sqrt{2\pi\sigma^2}} e^{-y^2/2\sigma^2}, \tag{1.3}$$

where $\sigma^2$is the variance of the single steps ΔX_n. From Eq. (1.2) one can read off the universal scaling relation

$$X_N \sim \sqrt{N} \tag{1.4}$$

for ordinary random walks. Alternatively one can compute the variance of X_N as a function of step number N,

$$\left\langle X_N^2 \right\rangle = \sigma^2 N. \tag{1.5}$$

Eq. (1.2) in combination with Eq. (1.3) implies that for large N the pdf $W_X(x, N)$ for the position X_N is asymptotically a spreading Gaussian:

$$W_X(x, N) \sim \frac{1}{\sqrt{N}} W_Y(x/\sqrt{N}). \tag{1.6}$$

The fact that $W_X(x, N)$ depends on the ratio $x/\sqrt{N}$ merely is another way of stating the scaling relation (1.4). Note however, that for relation (1.6) the existence of the variance of the single steps is no requirement as opposed to Eq. (1.5). On large scales trajectories of ordinary random walks resemble ordinary Brownian motion.

Lévy flights belong to a class of random walks for which the central limit theorem does not apply. They can be defined in a similar fashion as ordinary random walks, i.e. by a sum of independent identically distributed random increments (Eq. (1.1)). If the single step pdfs possess algebraic tails however, such that the single step second moment is divergent, i.e.

$$p(\Delta x) \sim \frac{1}{\Delta x^{1+\beta}} \qquad 0 < \beta < 2, \tag{1.7}$$

a generalization of the central limit theorem, the Lévy Khinchin theorem applies. It states that, if the position of a Lévy flight is scales according to

$$Y_N = \frac{X_N}{N^{1/\beta}}, \tag{1.8}$$

the scaled variable possesses a pdf independent of N in the limit $N \to \infty$, i.e.

$$\lim_{N\to\infty} W_{Y,\beta}(y, N) = W_{Y,\beta}(y). \tag{1.9}$$

The limiting density $W_{Y,\beta}(y)$ is referred to as a Lévy stable law of index β and is no longer Gaussian. It can be expressed most easily in Fourier-space:

$$W_{Y,\beta}(y) = \frac{1}{2\pi} \int \mathrm{d}k \, e^{-iky - D|k|^\beta}, \tag{1.10}$$

where D is some constant. Asymptotically, the limiting density has the same power law behaviour as the single step distribution,

$$W_{Y,\beta}(y) \sim \frac{1}{|y|^{1+\beta}}.$$

Combining Eqs. (1.8) and (1.10) one can obtain an explicit expression for the pdf of X_N in the limit of large step number,

$$W_{X,\beta}(x, N) \sim \frac{1}{N^{1/\beta}} W_{Y,\beta}\left(x/N^{1/\beta}\right).$$

This implies that the position of a Lévy flight scales superdiffusively with the step number:

$$X_N \sim N^{1/\beta}.$$

Geometrically, trajectories of Lévy flights are easily distinguished from those of ordinary Brownian motion. In Fig. 1.1 a two-dimensional trajectory of a Lévy flight is compared with a trajectory of ordinary Brownian motion.

1.2 Continuous time random walks

Temporally continuous random walks can be easily constructed from time discrete random walks by identifying the step number N with the time elapsed t and the associated time increment $\Delta t = t/N$ between successive steps. A generalization of this concept is the continuous time random walk (CTRW), a simple version of which is defined by two pdfs: one for the spatial displacements $f(\Delta x)$ and one for random temporal increments $\phi(\Delta t)$. The CTRW then consist of pairwise random and stochastically independent events, a spatial displacement Δx and a temporal increment Δt drawn from the combined pdf

$$p(\Delta x, \Delta t) = f(\Delta x)\phi(\Delta t).$$

After N iterations the position of the walker is given by

$$X_N = \sum_{n=1}^{N} \Delta x_n$$

and the time elapsed is

$$T_N = \sum_{n=1}^{N} \Delta t_n.$$

The quantity of interest is the position $X(t)$ after time t. The pdf $W(x,t)$ for this process can be computed in a straightforward fashion [1] and can be expressed in terms of the pdfs $f(\Delta x)$ and $\phi(\Delta t)$. The Fourier-Laplace transform of $W(x,t)$ is given by

$$W(k,u) = \frac{1-\phi(u)}{u\,(1-\phi(u)\,f(k))}, \tag{1.11}$$

where $\phi(u)$ and $f(k)$ denote the Laplace- and Fourier transform of $\phi(\Delta t)$ and $f(\Delta x)$, respectively. The pdf $W(x,t)$ is then obtained by inverse Laplace-Fourier transform

$$W(x,t) = \frac{1}{2\pi}\frac{1}{2\pi i}\int_{c-i\infty}^{c+i\infty} \mathrm{d}u \int \mathrm{d}k\, e^{ut-ikx} W(k,u). \tag{1.12}$$

$W(x,t)$ may exhibit four different universal behaviours which only depend on the asymptotics of $f(\Delta x)$ and $\phi(\Delta t)$ and thus the behaviour of $f(k)$ and $\phi(u)$ for small arguments.

1.2.0.1 Ordinary Diffusion

When both, the variance of the spatial steps and the expectation value of the temporal increments exist the Fourier- and Laplace transform of $f(\Delta x)$ and $\phi(\Delta t)$ read

$$\begin{aligned} f(k) &= 1 - \sigma^2 k^2 + \mathcal{O}(k^4) \\ \phi(u) &= 1 - \tau u + \mathcal{O}(u^2), \end{aligned}$$

where σ^2 and τ are some constants. Inserted into Eq. (1.11) and employing inversion (1.12) one obtains asymptotically

$$W(x,t) \sim \frac{1}{\sqrt{t}} e^{-x^2/Dt}.$$

Thus, CTRW are equivalent to Brownian motion on large spatio-temporal scales.

1.2.0.2 Lévy Flights

When the spatial displacements are drawn from a power-law pdf such as (1.7) the Fourier transform for small arguments is given by

$$f(k) = 1 - D_\beta |k|^\beta + \mathcal{O}(k^2).$$

When combined with temporal increments with finite expectation value, the same procedure as outlined above yields

$$W(x,t) \sim \frac{1}{t^{1/\beta}} L_\beta(x/t^{1/\beta}),$$

where L_β is a Lévy stable law of index β. Consequently, a CTRW with algebraically distributed spatial steps of infinite variance is equivalent to ordinary Lévy flights with a superdiffusive scaling with time

$$X(t) \sim t^{1/\beta}.$$

1.2.0.3 Fractional Brownian motion (subdiffusion)

The complementary scenario occurs when ordinary spatial steps (finite variance and $f(k) \approx 1 - \sigma^2 k^2$) are combined with a power-law in the pdf for temporal increments:

$$\phi(\Delta t) \sim \frac{1}{\Delta t^{1+\alpha}} \quad 0 < \alpha < 1.$$

In this case, the time between successive spatial increments can be very long, effectively slowing down the random walk. The Laplace transform for $\phi(\Delta t)$ is given by

$$\phi(u) = 1 - D_\alpha u^\alpha,$$

where D_α is some constant. One obtains for the position of such a random walk

$$W(x,t) = \frac{1}{2\pi} \int \mathrm{d}k e^{-ikx} E_\alpha(-D_\alpha k^2 t^\alpha), \tag{1.13}$$

where the function $E_\alpha$is the Mittag-Leffler function defined by

$$E_\alpha(z) = \sum_{n=0}^{\infty} \frac{z^n}{\Gamma(1+\alpha n)}.$$

It is easily checked that

$$W(x,t) \sim \frac{1}{t^{\alpha/2}} G_\alpha(x/t^{\alpha/2}),$$

where G_α is a non-Gaussian limiting function. From this the scaling relation

$$X(t) \sim t^{\alpha/2}$$

can be obtained. Since $\alpha < 1$ these processes are subdiffusive and sometimes referred to as fractional Brownian motion.

1.2.0.4 Ambivalent processes

The last and most interesting combination of waiting times and spatial steps is the one in which long waiting times compete and interfere with long range spatial steps, i.e. if both $\phi(\Delta t)$ and $f(\Delta x)$ decay asymptotically as a powerlaw:

$$f(\Delta x) \quad \sim \quad \frac{1}{\Delta x^{1+\beta}} \qquad 0 < \beta < 2$$

and

$$\phi(\Delta t) \sim \frac{1}{\Delta t^{1+\alpha}} \qquad 0 < \alpha < 1.$$

In this case

$$\begin{aligned} f(k) &= 1 - D_\beta |k|^\beta + \mathcal{O}(k^2) \\ \phi(u) &= 1 - D_\alpha u^\alpha + \mathcal{O}(u^2). \end{aligned}$$

The asymptotic pdf for the position of the ambivalent process can again be expressed in terms of a Fourier inversion and the Mittag-Leffler function according to

$$W(x,t) = \frac{1}{2\pi} \int \mathrm{d}k e^{-ikx} E_\alpha(-D_\alpha |k|^\beta t^\alpha). \tag{1.14}$$

Note, however, the term $|k|^\beta$in the argument of E_α. From Eq. (1.14) one can extract the scaling relation

$$X(t) \sim t^{\alpha/\beta}.$$

The ratio of the exponents α/β resembles the interplay between sub- and superdiffusion. For $\beta < 2\alpha$ the ambivalent CTRW is effectively superdiffusive, for $\beta > 2\alpha$ effectively subdiffusive. For $\beta = 2\alpha$ the process exhibits the same scaling as ordinary Brownian motion, despite the crucial difference of infinite moments and a non-Gaussian shape of the pdf $W(x,t)$.

The various types of asymptotic universal behaviours are depicted in Fig. 1.2 which shows a phase diagram spanned by the temporal exponent α and the spatial exponent β.

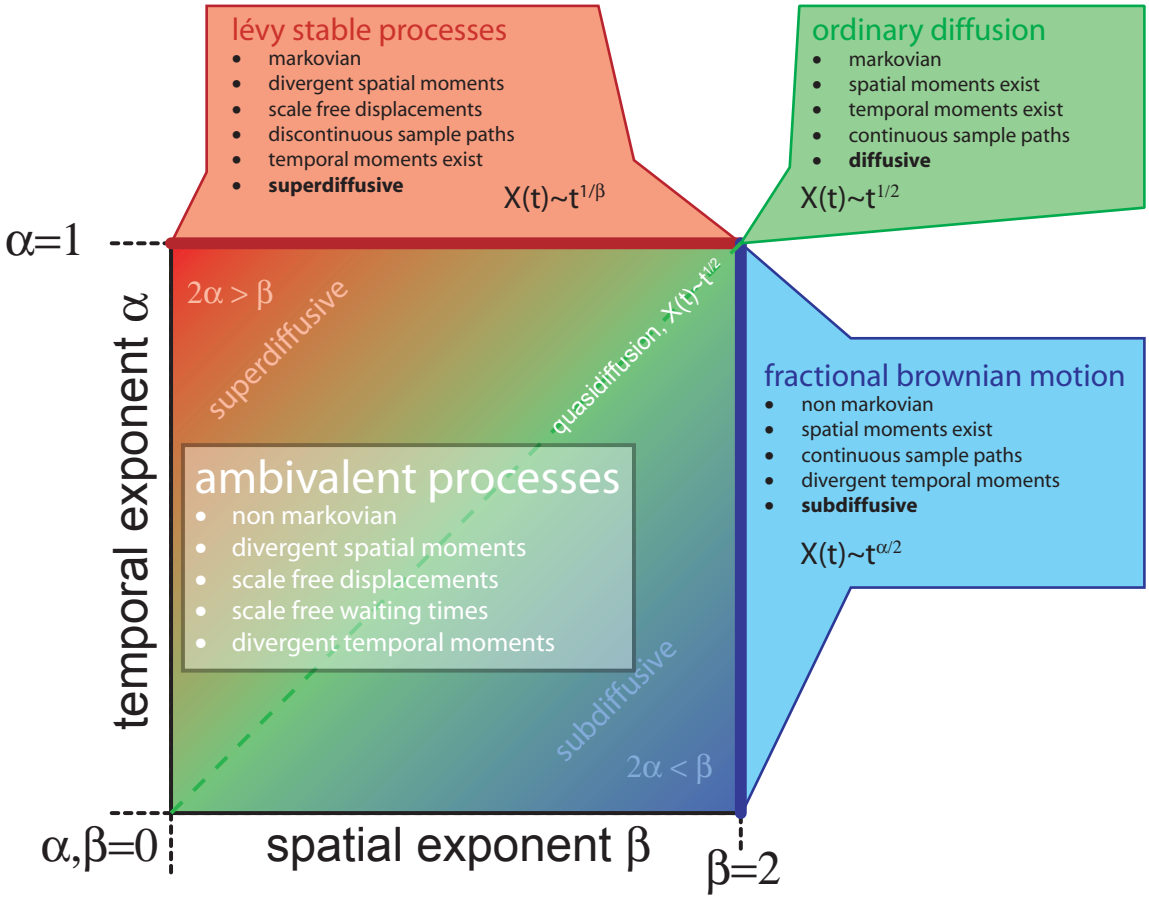

Figure 1.2: The asymptotic universality classes of continuous time random walks defined in the text as a function of the universality exponents $0 < \alpha < 1$ and $0 < \beta < 2$. Lévy flights, fractional Brownian motion as well as ordinary diffusion are limiting cases of the more general class of ambivalent processes.

Bibliography

[1] Ralf Metzler and Joseph Klafter, *The random walks guide to anomalous diffusion: A fractional dynamics approach*, Phys. Rep. **339** (2000), 1–77.

1 Relaxation time estimate for Lévy flights in a confined two dimensional region

One can estimate the time to reach equilibrium for a two-dimensional Lévy flight in a confined region of linear extent L as follows. Assume that the single step radial distribution of the random walk can be approximated by

$$p_{\Delta t}(\mathbf{x}) = (1-Q)\delta(\mathbf{x}) + Q\, f_{\delta L}(\mathbf{x}). \tag{1.1}$$

Here Δt denotes the typical time between single steps, Q the fraction of walkers which jump a distance $d > \delta L$ and $(1-Q)$ the fraction which remains in a disk defined by $|\mathbf{x}| \leq \delta L$. The function $f_{\delta L}(\mathbf{x})$ comprises the power-law in the single steps, characteristic for Lévy flights:

$$f_{\delta L}(\mathbf{x}) = C\,\delta L^{\beta} |\mathbf{x}|^{-(1+\beta)} \qquad |\mathbf{x}| \geq \delta L.$$

Inserting this into Eq. (1.1) one obtains that $f_{\delta L}(\mathbf{x})$ is normalized to unity and that the normalization constant C is independent of the microscopic length δL. The Fourier-transform of $p(\mathbf{x})$ is given by

$$\tilde{p}(\mathbf{k}) = (1-Q) + Q\tilde{f}_{\delta L}(\mathbf{k}).$$

The Fourier-transform of the probability density function $W_N(\mathbf{x})$ of the walker being located at a position $\mathbf{x}$ after N steps can be computed in terms of $\tilde{p}(\mathbf{k})$ according to

$$\tilde{W}_N(\mathbf{k}) = \tilde{p}(\mathbf{k})^N \approx \left(1 - Q\delta L^{\beta}|\mathbf{k}|^{\beta}\right)^N \approx e^{-QN\,|\delta L\,\mathbf{k}|^{\beta}}. \tag{1.2}$$

The relaxation time in a confined region is provided by the lowest mode

$$k_{\text{min}} = \frac{L}{2\pi}.$$

Inserted into (1.2) with $N = t/\Delta t$ on obtains

$$T_{\text{eq}} \approx \delta T/Q\,(L/2\pi\delta L)^{\beta}\,.$$

1 The mechanisms underlying the spread of disease and bank notes

The similarities between the geographical spread of infectious diseases and of bank notes are illustrated in Fig. 1.1. Humans possess home ranges, which can be operationally defined as a geographical patch in which a person resides most of the time. Humans interact and pass a disease by virtue of overlapping home ranges or travelling to a home range belonging to someone else. The temporal succession of steps involved in an idealized model for the spread of disease are the following. An infected person (red) visits a susceptible individual (blue) and transmits the disease. Subsequently the initially infectious person returns to his or her home range (forward geographical transport A in Fig. 1.1). Alternatively a susceptible person (purple) can visit an infected one and take home the disease (backward geographical transport). Money is transported along the same pathways as indicated in the figure. The symmetry of the system suggests that both pathways possess identical probability density functions for the distance traveled.

On small length scales (the size of a few patches in the model) and temporal scales (a small number of transmissions) the characteristics of disease transport on one hand and bank note transport on the other may differ. The limiting theorems of random walks (see supplementary information on Lévy flights and continuous time random walks), however, suggest that on large spatio-temporal scales the distribution of travelling distances of both disease and bank notes share universal characteristics which determine the geographical spread.

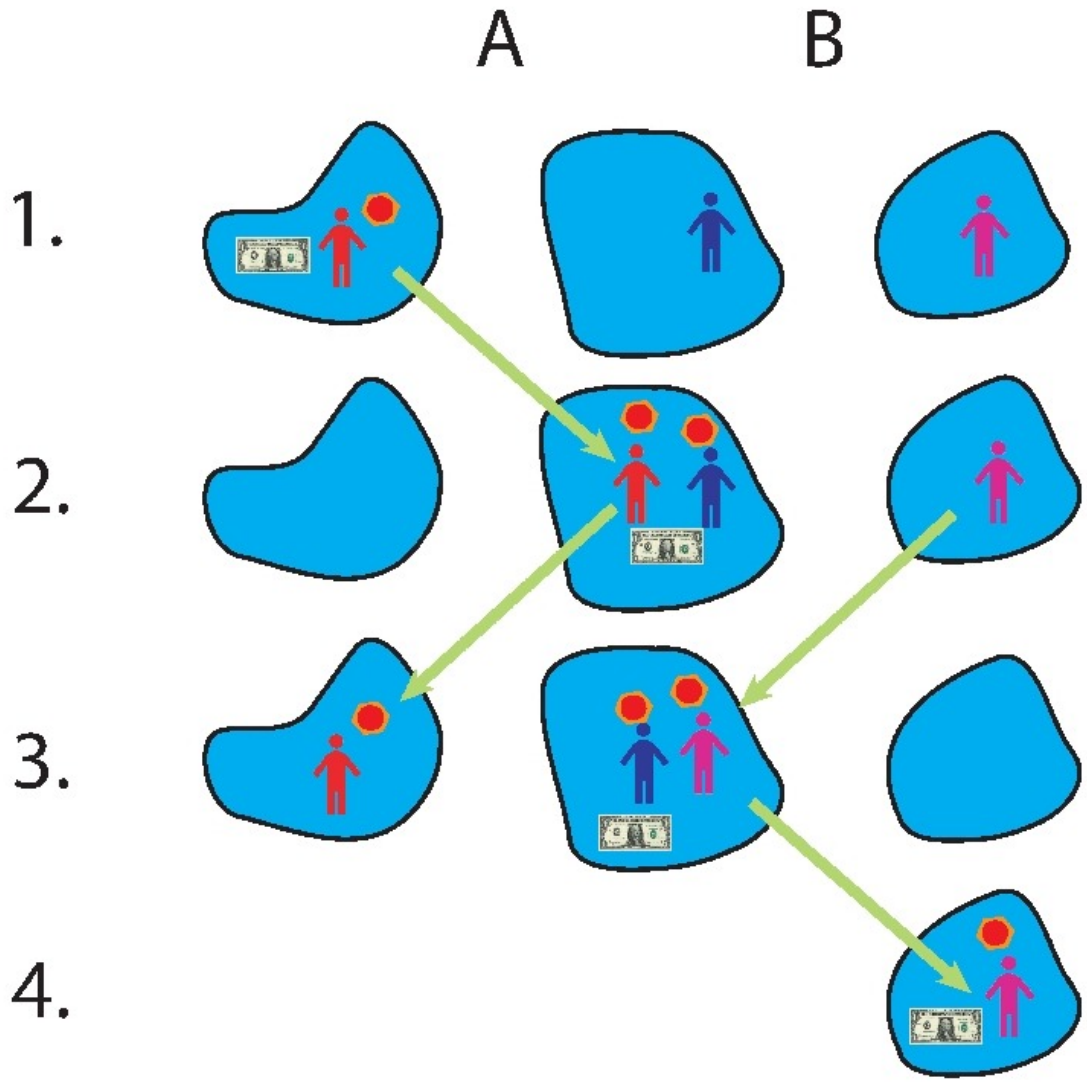

Figure 1.1: Qualitative mechanisms of the geographical spread of disease and bank notes. The numbers on the left indicate the temporal succession of steps involved. The blue areas indicate home ranges of three individuals. The spread can occur along pathways A and B. In A an infected individual leaves his or her home range and visits a susceptible person (blue) which is subsequently infected. The initially infectious person returns home. A third susceptible person (purple) visits the newly infected person (blue), is infected and returns with the disease (pathway B). As indicated, bank notes travel in a qualitatively similar fashion.